ZANCO Journal of Pure and Applied Sciences

TYPE Original article
DOI http://dx.doi.org/10.21271/ZJPAS.37.6.3

OPEN ACCESS

*Corresponding author
Yasir Hussein Mohammed
yasir.h.m@uomosul.edu.iq

RECEIVED :07 /05 /2025
ACCEPTED :28/06/ 2025
PUBLISHED :31/ 12/ 2025

KEYWORDS:
CVD; ZnO-TFs; ZnO NRs; optical characteristics; morphological analysis.

Controlling ZnO Nanorods Morphology by Seeded Layer Assisted Chemical Vapor Deposition

Mithaq Ali Salih and Yasir Hussein Mohammed*

Department of Physics, College of Education for Pure Science, University of Mosul, 41002 Mosul, Iraq.

ABSTRACT

Vertically aligned zinc oxide (ZnO) nanorods (NRs) were grown using a seeded layer-assisted chemical vapor deposition technique. This study examined the impact of altered evaporation crucible-substrate spacing (3, 4, 5, and 6 cm) on the optical behavior, morphological characteristics, and elemental composition of ZnO thin films prepared as a seed layer (buffer layer). Besides, the surface morphology and structural characteristics of the synthesized ZnO NRs was evaluated in the presence and absence of the seed layer. Seed layer samples were evaluated by an ultraviolet-visible spectrophotometer, a field emission scanning electron microscope (FESEM), and energy-dispersive X-ray (EDX) spectroscopy. In contrast, the NRs samples were characterized using FESEM and X-ray diffraction (XRD) technique. The optical energy gap results showed a blue shift from 3.23 eV to 3.28 eV as the separation spacing increased from 3 cm to 6 cm, respectively. FESEM images revealed that the separation spacing strongly influences the morphology of the ZnO films. EDX analysis of the seed layer disclosed the presence of prominent peaks for zinc and oxygen, which confirmed the elemental composition of the grown samples. Furthermore, ZnO NRs synthesized in the absence of a seed layer were observed to be shorter, misaligned, exhibit random growth rates, and possess inferior quality compared to those synthesized with a seed layer. XRD analysis confirmed the high crystalline quality of the grown nanorod samples. Our systematic technique for the synthesis and characterization of the seed layer could play a significant role in the production of superior nanorod arrays.

1.Introduction

Thin films (TFs), which are layer of material with thicknesses ranging from nanometers (nm) to micrometers (μm), have become essential in modern technology, enabling a wide range of applications in sectors like energy conversion, energy storage, and electronics. The unique characteristics of TFs, like their ability to be controlled and easily tailored, have motivated the quick development of various fabrication systems, both chemical and physical, each with its own advantages and applications [1-4]. TFs deposition techniques have progressed significantly, allowing the production of a diverse array of devices and structures, including solar cells, smart coatings, and integrated circuits. In addition to the thin films morphologies, ZnO has also been found to have a broad range of growth morphologies, including nanoparticles, nanotubes, NRs, nanoneedles, nanowires, nanocages, nanotetrapods, nanohelix, nanorings, and nanocombs [5]. The deposition methods and variations in growth conditions (temperature, pressure, growth time, gas flow rate, position, etc.) are considered the main causes of these different types of morphologies [6-8]. ZnO nanostructures (NSs) have gained wide attention for numerous useful applications, such as solar cells [9], biosensor [10], piezoelectric nanogenerators [11], light-emitting diodes [12], UV photodetection [13], marine antifouling systems [14], photodetector device [15], and so on. These applications can only be activated by controlling the physical and chemical properties of the grown material. ZnO can be considered an exceptional material for use in the aforementioned applications owing to its wide optical energy gap (E_g=3.37 eV), high excitation binding energy (60 meV), have a hexagonal wurtzite structure, and high mechanical and thermal stability [16]. ZnO as a seed layer, acting as a nucleation center for the growth of one dimensional (1D) ZnO NSs, has a strong impact on their physical characteristics [17]. Additionally, previous studies have highlighted the significance of a seed layer in the fabrication of the ZnO NRs [18]. The results indicate that ZnO NRs produced from a seed layer via sol-gel methods exhibit superior quality compared to those grown without a seed layer [18]. A different investigation by Fang's group shows that ZnO NRs cannot be directly synthesized from silicon-based materials [16]. Findings from another research effort suggest that the thickness of the seed layer can influence the alignment of ZnO NRs [19]. An increased thickness of the seed layer leads to misaligned ZnO NRs, while a reduced thickness promotes vertical alignment and high density of the ZnO NRs [19]. Therefore, it is determined that the thickness of the seed layer plays a significant role in the growth of the ZnO NRs. There is a general consensus that this layer functions as a framework for the growth of NRs. However, the condition of the ZnO seed layer can be tuned through growth techniques and their related growth parameters (temperature [16], precursor concentration [20], annealing temperatures [21]). The well-aligned and controlled growth of 1D ZnO NSs is a key issue in many optoelectronic applications. The main issues for the well-aligned vertical growth of 1D ZnO NSs are an ultrathin film and uniform distribution of the ZnO seed in the ZnO film. A range of fabrication methods has been utilized to create the ZnO seed layer [17, 18]; however, the complex nature of the necessary machinery results in elevated expenses, making these approaches unfeasible for the large-scale manufacturing of ZnO seed layer [21]. In addition, there has been less focus on the chemical route technique known as chemical vapor deposition (CVD) at atmospheric pressure (AP).

Taking into consideration these essential factors, the current research aspires to explain the impact of the changed evaporation crucible-substrate spacing (3, 4, 5, and 6 cm) on the optical behavior, morphological characteristics, and elemental composition of ZnO TFs prepared as a seed layer. Besides, the surface morphology and structural characteristics of the grown ZnO NRs was evaluated in the presence and absence of the seed layer. The deposition films were characterized by ultraviolet-visible (UV-Vis) spectrophotometer, FESEM, and EDX spectroscopy. In contrast, the NRs samples were characterized using FESEM and XRD.

2. Experimental details

The process was conducted in two steps: (i) the formation of a ZnO seed layer, and (ii) the growth of the ZnO NRs.

2.1 ZnO seed layer deposition

In this investigation, a thin layer of ZnO was synthesized to act as a seed layer using the CVD method at atmospheric pressure on standard glass substrates sized 1 cm × 1 cm, with different gaps of 3, 4, 5, and 6 cm between the evaporation crucible and the glass substrates. Fig. 1 illustrates the diagram of the APCVD setup, which is fundamentally composed of a gas delivery scheme, deposition reactor, and exhaust gas treatment unit. Initially, the glass substrates underwent ultrasonic cleaning with acetone, ethanol, and deionized (DI) water for approximately 10 minutes in each liquid to eliminate any impurities (fats, dust, etc.) and then dried with a hot air stream [22]. Following a cleaning process, the glass substrates and an alumina crucible (4 cm× 1 cm) containing 1 g of zinc (Zn) acetate dihydrate ($(CH_3COO)_2$ $Zn.2H_2O$ (ZAD), 99.97%) powder as base material were positioned on a smooth stainless steel platform and then transferred into the miniature quartz tube. Then, a miniature quartz tube (20 cm in length and 5 cm in diameter) was inserted into the center of the larger tube (deposition reactor) with a diameter of 6.5 cm, where the temperature was adjusted to 425 °C. This unique arrangement allows the smaller reaction tube to trap vapor, creating an environment with a high concentration of Zn within the quartz tube. After securely fastening the quartz tube with a sealing flange assembly, the heating procedure was carried out. At the temperature of evaporation, oxygen (O_2) gas was fed into the reactor at a flow rate of 200 sccm, carefully measured by mass flow controllers. The growth duration continued for 15 minutes under a pressure of 760 Torr. Throughout the growth process, all other growth factors were maintained at a constant and carefully regulated state. Finally, once the furnace had naturally cooled to ambient temperature, the samples are extracted from the reactor for analysis.

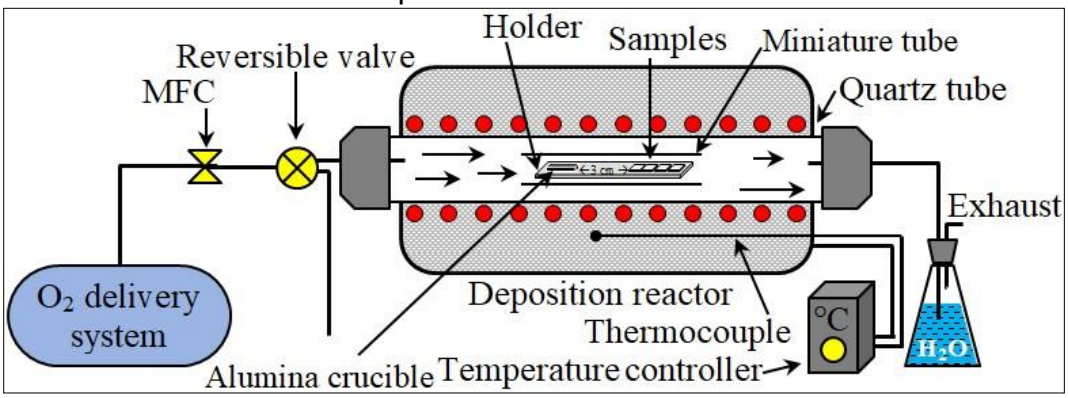

Fig. 1. Schematic representation of the CVD approach.

2.2 ZnO nanorods growth

To understand the impact of the seed layer, ZnO NRs were grown on two different glass substrates (one with a seed layer and the other without) using a two-zone CVD method at atmospheric pressure. An optimum thickness of a seed layer (178 nm thick) was used to grow the ZnO NRs. The two substrates were positioned on a stainless-steel holder inclined at 14° and then placed into the deposition reactor within heating zone II, where the growth temperature was maintained at 600 ± 5 °C. Subsequently, an alumina crucible filled with 1.6 g of ZAD powder was placed into reactor heating zone I and heated until it reached an evaporation temperature of 250 ± 10 °C. A spacing of 5 cm was maintained between the substrates and the crucible. O_2 gas was introduced into the reactor at the evaporation temperature, flowing at a rate of 25 sccm, which was carefully controlled using mass flow regulators. The growth procedure continued for 1 h. A trial-and-error technique was employed to determine the optimum conditions for growing high-quality ZnO NRs, such as the

growth temperature, type of precursor, gas flow rate, quartz tube dimensions, boat-to-substrates spacing, substrate alignment, room temperature, etc [6, 7, 23].

By a UV-Vis spectrophotometer (Shimadzu UV-1800, Japan), the optical transmittance and absorbance spectra of the samples were analyzed within the wavelength interval of 360 to 1100 nm, employing a plain glass as a reference standard. The estimated thickness of grown structures was measured by the microbalance method [24] through the formula: $\mathrm{t\,(cm)} = (\Delta m\,(\mathrm{gm})/\mathrm{A}\,(\mathrm{cm}^2)\,\rho(\mathrm{gm/cm}^3))$, where $\Delta m = (m_2 - m_1)$ represents the mass difference before (m_1) and after deposition (m_2), A is the area of the sample, and ρ is the density of the ZnO material (5.61 gm/cm³). The samples' surface morphology was investigated with the aid of a FESEM (inspect f 50-FEI). Using the same microscope, we conducted an elemental analysis of the samples via EDX spectroscopy. XRD analysis of the grown ZnO NRs was conducted in the range of 10°-80° using a XRD Panalytical X'pert Pr with Cu Kα radiation (λ = 1.5406 Å) at a voltage of 40 kV and a current of 30 mA.

3. Results and discussion

Fig. 2 shows the optical transmittance spectra of ZnO-seeded glass substrates deposited with different evaporation crucible-substrate spacing. From Fig. 2 we can see that tuning the APCVD technique parameters conditions can influence the uniformity and thickness of the resulting seed layers. It is important to note that the grown samples show varying thicknesses. This behavior may be attributed to differences in the distance between the evaporation crucible and the glass substrates. The thicknesses of the samples prepared at 3, 4, 5, and 6 cm were measured to be 891, 623, 535, and 178 nm, respectively. Clearly, films created at a distance ≥ 5 cm exhibit high transparency in both the visible and infrared regions due to their inherent absorption characteristics [25]. For ≤ 4 cm, the average transmittance of the samples decreased (see Fig. 2). Various elements, including the presence of impurities, lack of oxygen, the thickness of the film, quality of the crystal structure, and roughness of the surface, influence metal oxides' ability to transmittance light [6, 7, 23]. This decrease in optical transmittance in our case may be due to increase in the film thickness. Furthermore, the reduction in the optical transmittance may be due to light scattering caused by the rough surface of the samples. Generally, films with high metal content (see Fig. 2, 3 cm and 4 cm) tend to be more opaque [26]. In summary, ZnO-seeded substrates of small thicknesses have the optimal thickness for the growth of the ZnO NRs [19].

Fig. 3 depicts the optical absorbance spectra of ZnO-seeded glass substrates prepared with different evaporation crucible-substrate spacing. The prepared samples revealed that spacing significantly affects their absorbance spectra. A clear absorption edge was detected in the 360-400 nm interval, corresponding to the optical E_g. The reduced transmittance in the UV spectrum (less than 380 nm) is due to the intense absorption in this area (see Fig. 3), which arises from the large E_g of ZnO films. The strong absorption of ultraviolet light, which features low reflection, was confirmed for the transition of electrons from the valence band to the conduction band [27]. The recorded transmittance information can be used to derive the absorption coefficient (α) of the samples, following the guidelines of the Beer-Lambert law [28].

$$\alpha\,(\mathrm{cm}^{-1}) = -(\ln(\mathrm{T})\,/t), \qquad (1)$$

Here, the term transmittance (T) is expressed as T% divided by 100, and (t) refers to the thickness of the fabricated ZnO TFs.

Fig. 4 presents the absorption coefficient spectra of ZnO-seeded glass substrates prepared with different evaporation crucible-substrate spacing. From Fig. 4, the value of the absorption coefficient of the grown samples in the UV area (<400 nm) increased from ~1.65×10^5 cm^{-1} to ~3.34×10^5 cm^{-1} with spacing increasing from 3 cm to 6 cm. Samples created with a spacing of 6 cm show a strong absorption coefficient in the ultraviolet spectrum.

Conversely, samples prepared with a spacing of 5 cm or less demonstrated a notable decrease in their absorption coefficient within the same UV range. This behavior may be ascribed to the variation in the crystallites size [7]. In order to determine the direct optical E_g of the synthesized samples, we utilized Tauc's equation in the region of high absorbance as outlined below [29]:

$$\alpha h\nu = A(h\nu - E_g)^n, \qquad (2)$$

In this equation, hv represents the energy of the photon, A denotes Tauc's constant, and n equals 1/2 for a direct allowed transition.

Fig. 5 displays $(\alpha hv)^2$ VS. (hv) graphs of ZnO-seeded glass substrates prepared with different evaporation crucible-substrate spacing. Provided that E_g is equal to hv at the point where $(\alpha hv)^2$ is zero, projecting the linear portion of the graph (see Fig. 5) onto the x-axis reveals the value of E_g. For the samples prepared at 3, 4, 5, and 6 cm, the optical E_g were determined to be 3.23, 3.24, 3.27, and 3.28 eV, respectively. The value of E_g increased from 3.23 eV to 3.28 eV with the spacing increasing from 3 cm to 6 cm, and the optical absorption edge exposed a blue shift (shift towards higher energy). Fig. 5 indicates that decreasing film thickness increases the E_g from 3.23 eV to 3.28 eV due to decreased lattice defects [30]. Typically, the E_g exhibits a high sensitivity to variations in film stress, the concentration of free carriers, film thickness, and the arrangement of grain boundaries [31, 32]. Thus, the optical E_g of the ZnO film is influenced by the films thickness. Besides, the values of the optical transmittance and E_g confirm the applicability of the ZnO films as efficient films in different optoelectronic applications [23, 25].

Growth of the ZnO NRs by various techniques requires a seed layer from ZnO films, which should have a continuous and smooth surface with low thickness, to achieve high-quality ZnO NRs. Fig. 6 illustrates FESEM images of ZnO-seeded glass substrates prepared with different evaporation crucible-substrate spacing. The morphological characteristics of ZnO films were observed to be significantly influenced by the distance separating the evaporation crucible from the glass substrates. At short spacing of 3 cm (see Fig. 6a), atoms arrive quickly with high flow, resulting in rapid and irregular aggregation (nucleation) at specific locations on the substrate surface. This leads to increased roughness of the surface layer of deposited films. These outcomes align well with optical transmittance data (see Fig. 2). At a medium spacing of 4 to 5 cm (see Fig. 6b and c), the vapor flow is moderate, allowing atoms sufficient time to diffuse across the substrate surface before bonding. In this case, the atoms may be distributed evenly, producing small grains with low roughness. With an increase in the spacing to 6 cm (see Fig. 6d), the growth of ZnO films became more regular, making the surface of the films smoother. However, a thinner ZnO seed layer results in a larger surface area of the deposited films because of the smaller crystallite size of these films, which positively affects the growth of 1D nanomaterials [33]. Moreover, FESEM analyses have verified the presence of nanocrystalline structures within the synthesized films. Finally, the adhesion of the ZnO TFs deposited on the glass substrates at 425 °C was excellent, as demonstrated by the scratch test.

The EDX technique was exploited to determine the purity and atomic ratios of Zn and O within the prepared films. Fig. 7 exhibits EDX spectra of ZnO-seeded glass substrates prepared with different evaporation crucible-substrate spacing. It is observed from the spectra (see Fig. 7) that the grown films mainly consist of Zn and O element. The minor peaks present in the spectrum such as Mg, Al, Si, Ca, K, Fe, and Ni can be attributed to the commercial glass substrates used [34]. The C signal arises from the carbon tape that has been secured to the holder of the sample [35, 36]. This displays that the elements dominated by the ZnO films were pure ZnO. However, the atomic ratio of Zn decreased from 16.2 to 7.8 as the spacing increased from 3 cm to 6 cm (i.e., the thickness of the films decreased). The outcomes were consistent with the findings from the optical assessment. Further, one can clearly observe

that the thickness of the film plays a crucial role in determining its stoichiometry (see inset tables in Fig. 7). For all samples, the Zn/O ratio was smaller than unity (see inset tables in Fig. 7), revealing that the total O content was higher than that of Zn in the grown samples. The adsorbed excess O forms and hydroxides can contribute to the increase in the oxygen content detected by EDX [34]. In addition, prior investigations revealed that obtaining precise measurements of O via EDX is problematic due to the presence of O in the SiO_2 substrate (glass substarte) [37].

To enhance the understanding of the chemical structure of the ZnO films across different samples, a chemical mapping technique was utilized to investigate the distribution and composition of the atomic elements. Fig. 8 portrays EDX mapping of ZnO-seeded glass substrates prepared with different evaporation crucible-substrate spacing. In Fig. 8, each square elucidates the distribution of a particular element in the grown sample, and the colors indicate the concentration of the element, where light or bright colors (such as yellow or light green) indicate higher concentrations. In contrast, darker colors indicate an absence or lower concentration of the element. The columns in Fig. 8 show a chemical mapping for O (yellow-green), C (green), Ca (purple), Zn (greenish-cyan), Si (orange), Fe (dark blue), K (magenta), Mg (dark red), Ni (red), Al (violet), atoms. The chemical mapping for C, Fe, K, Mg, Ni, and Al atoms is not shown here in Fig. 8 for brevity. In general, the distribution of main atomic elements (Zn and O) on the substrates was excellent, indicating the high efficiency of the technique used for fabricating the samples.

Fig. 9 displays FESEM images of the ZnO NRs grown without and with the ZnO seed layer. As shown in Fig. 9, the surface morphology of the ZnO NRs strongly depended on the seed layer. ZnO NRs grown without a seed layer (see Fig. 9a) showed somewhat poor vertical alignment with short lengths and a non-uniform growth rate. In contrast, vertically well-aligned ZnO NRs were grown on ZnO-seeded glass substrates with longer lengths and a uniform growth rate, as shown in Fig. 9b. Finally, by controlling the properties of the seed layer, the ZnO nanorods morphologies and growth rate can be changed. However, the enhanced control of the morphology of the ZnO NRs may lead to an improved collection of carriers in ZnO-based hybrid polymer solar cells [19]. Based on FESEM images, the growth approach is founded on the vapor-solid (VS) mechanism, which involves the condensation and oxidation of metal vapor on a hot substrate surface, allowing the metal to function as a self-catalyst for nanostructure growth [7]. Using ImageJ software (version 1.47v), the dimensions of the ZnO NRs were methodically assessed by analyzing FESEM images. The results revealed that the synthesized nanorods had sizes ranging from 159 to 755 nm, indicating a uniform distribution of diameters [6, 7]. As demonstrated by this analysis, the regularity in the dimensions of nanorods is important for achieving reliable outcomes in their intended uses, particularly in sensing equipment and solar panels, where the regularity of dimensions directly affects charge transport properties.

Fig. 10 reveals the XRD patterns of the ZnO NRs grown without and with the ZnO seed layer. XRD analysis reveals prominent peaks at 2θ angles of (31.92°), (34.76°), (36.6°), (63.12°), and (72.84°), which align with the (100), (002), (101), (103), and (004) crystal planes of hexagonal wurtzite ZnO, as indicated by JCPDS card number 36-1451. The sharp and intense diffraction peak related to the (002) plane, with a narrow full-width at half-maximum (FWHM) of 0.16410°, confirms that the grown nanorods exhibit a high level of crystallinity. However, the absence of peaks associated with impurities offers further assurance regarding the purity of the phases in synthesized samples. Finally, these findings complement current electron microscopy observations and provide conclusive evidence of the wurtzite crystal arrangement in the synthesized nanorods.

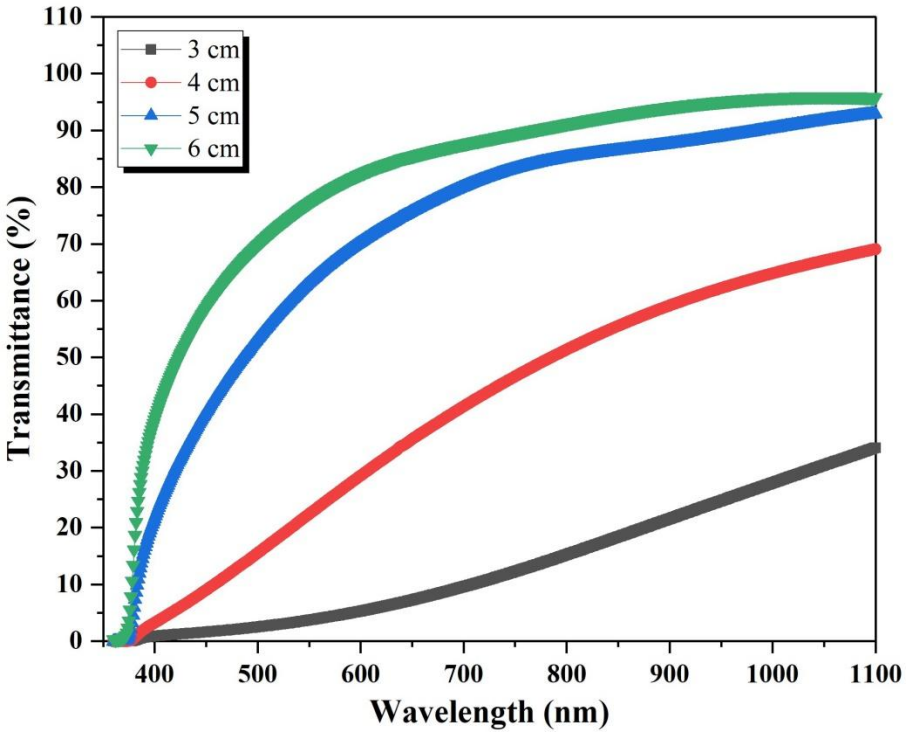

Fig. 2. Optical transmittance spectra of ZnO-seeded glass substrates deposited with different spacing from the evaporation crucible.

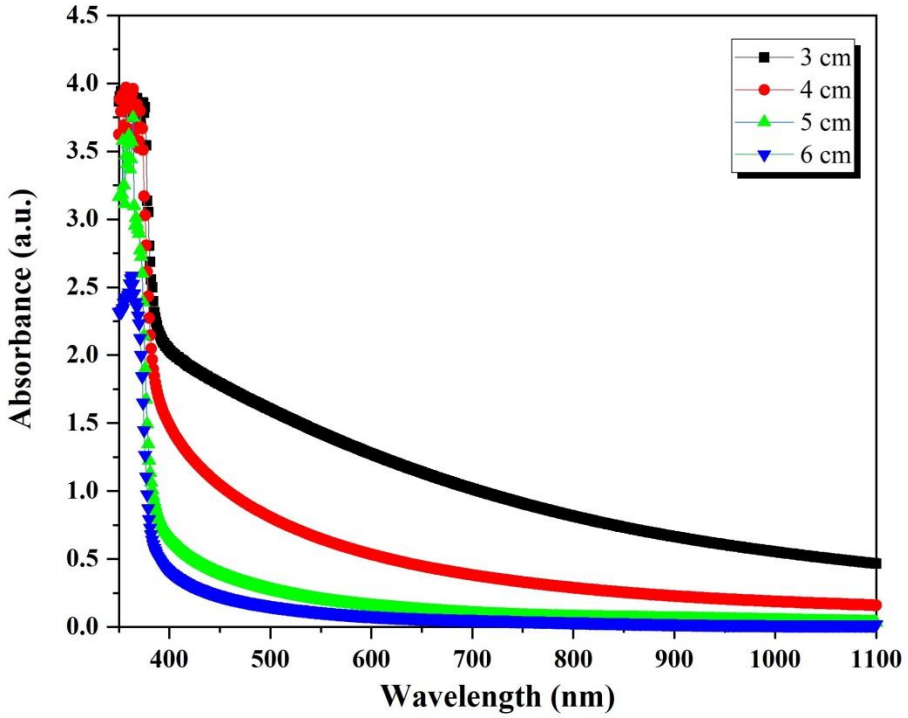

Fig. 3. Optical absorbance spectra of ZnO-seeded glass substrates prepared with different spacing from the evaporation crucible.

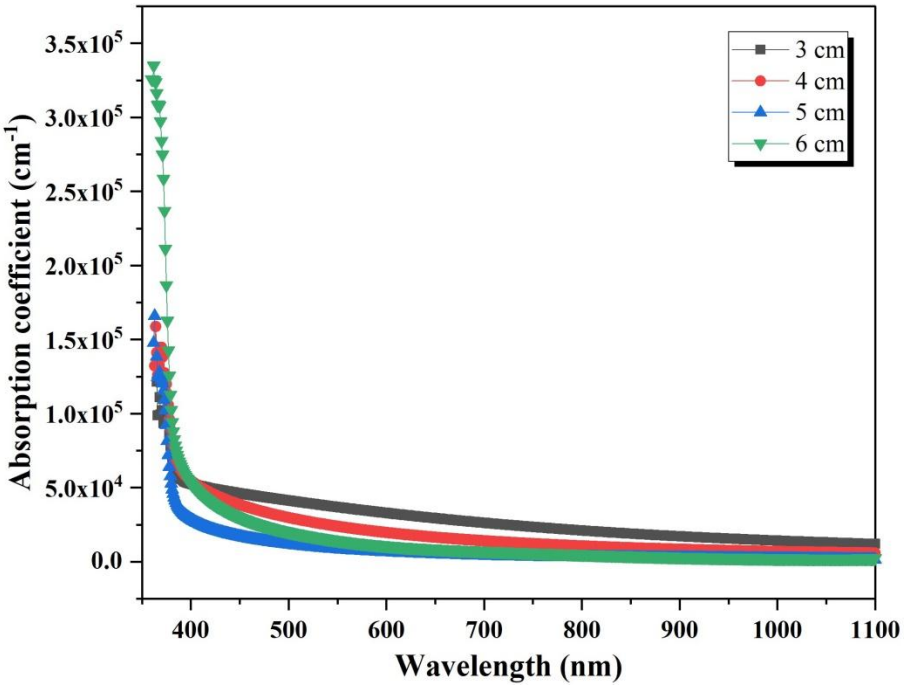

Fig. 4. Absorption coefficient spectra of ZnO-seeded glass substrates produced with different spacing from the evaporation crucible.

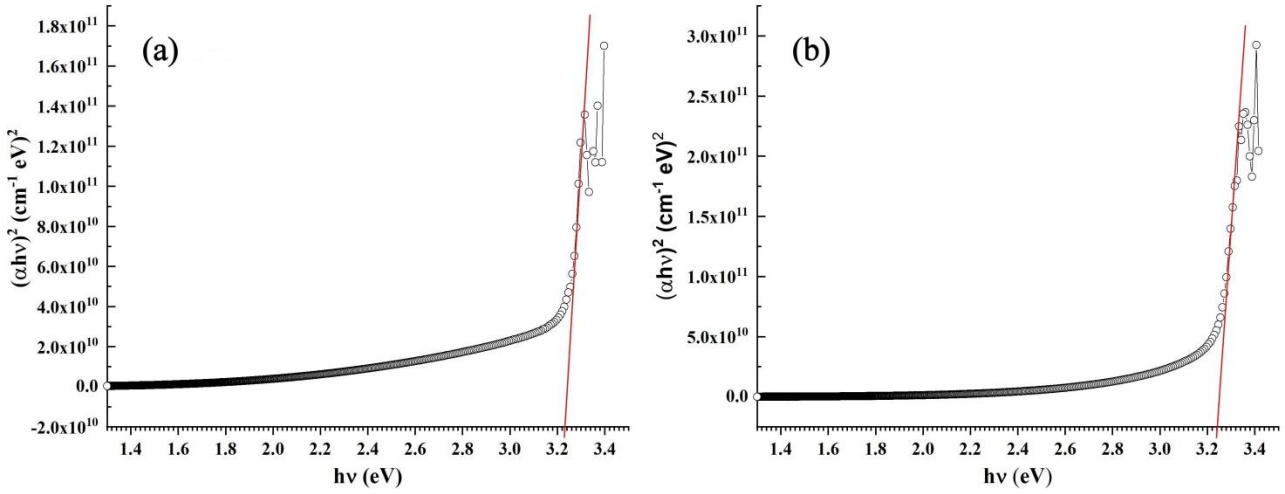

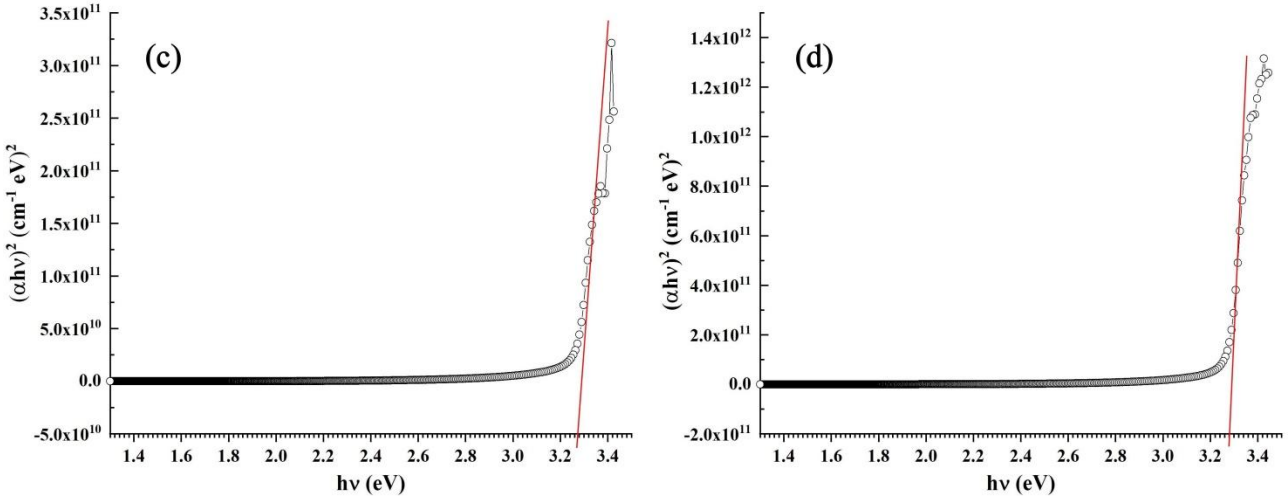

Fig.5. The relationship between $(\alpha hu)^2$ and (hu) of ZnO-seeded glass substrates prepared with different spacing from the evaporation crucible (a) 3 cm, (b) 4 cm, (c) 5 cm, and (d) 6 cm.

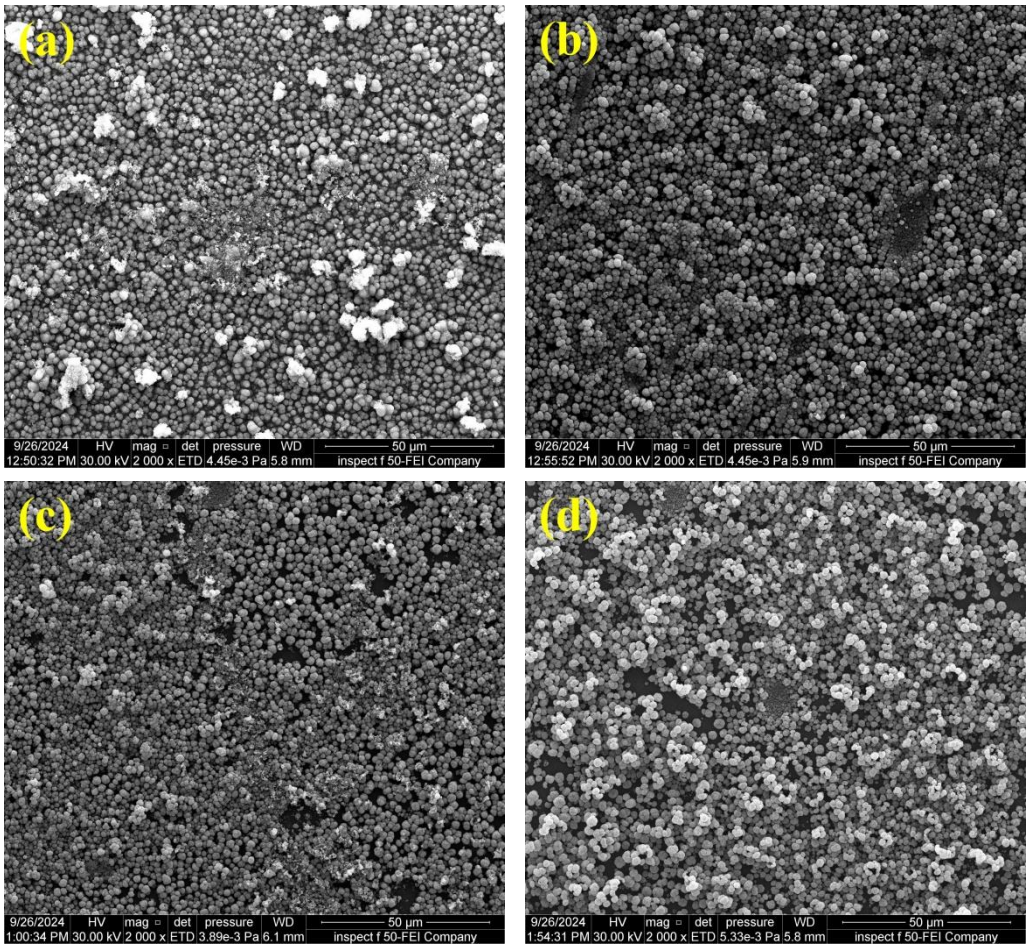

Fig. 6. FESEM images of ZnO-seeded glass substrates prepared with different spacing from the evaporation crucible (a) 3 cm, (b) 4 cm, (c) 5 cm, and (d) 6 cm.

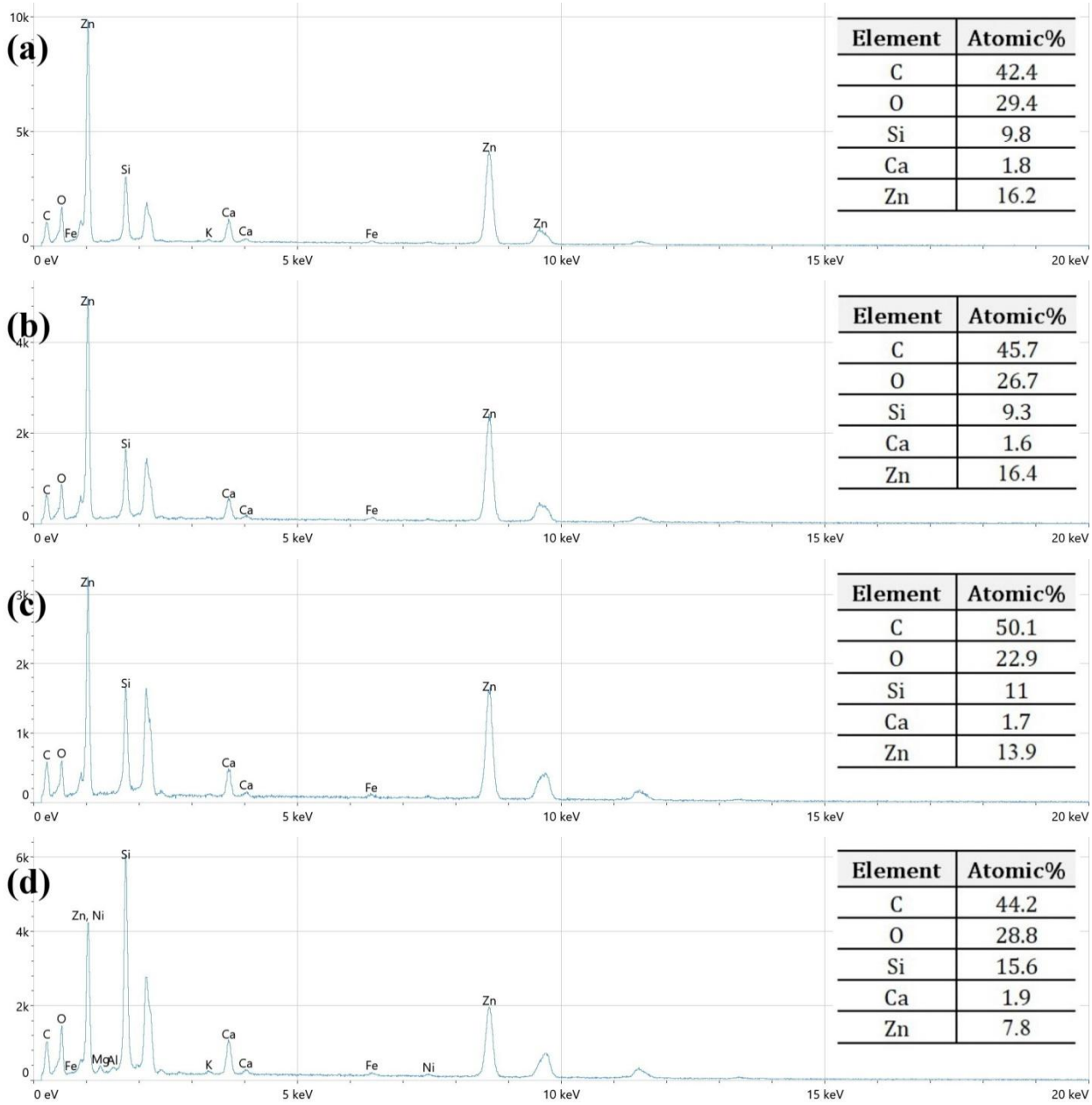

Fig. 7. EDX spectra of ZnO-seeded glass substrates prepared with different spacing from the evaporation crucible (a) 3 cm, (b) 4 cm, (c) 5 cm, and (d) 6 cm.

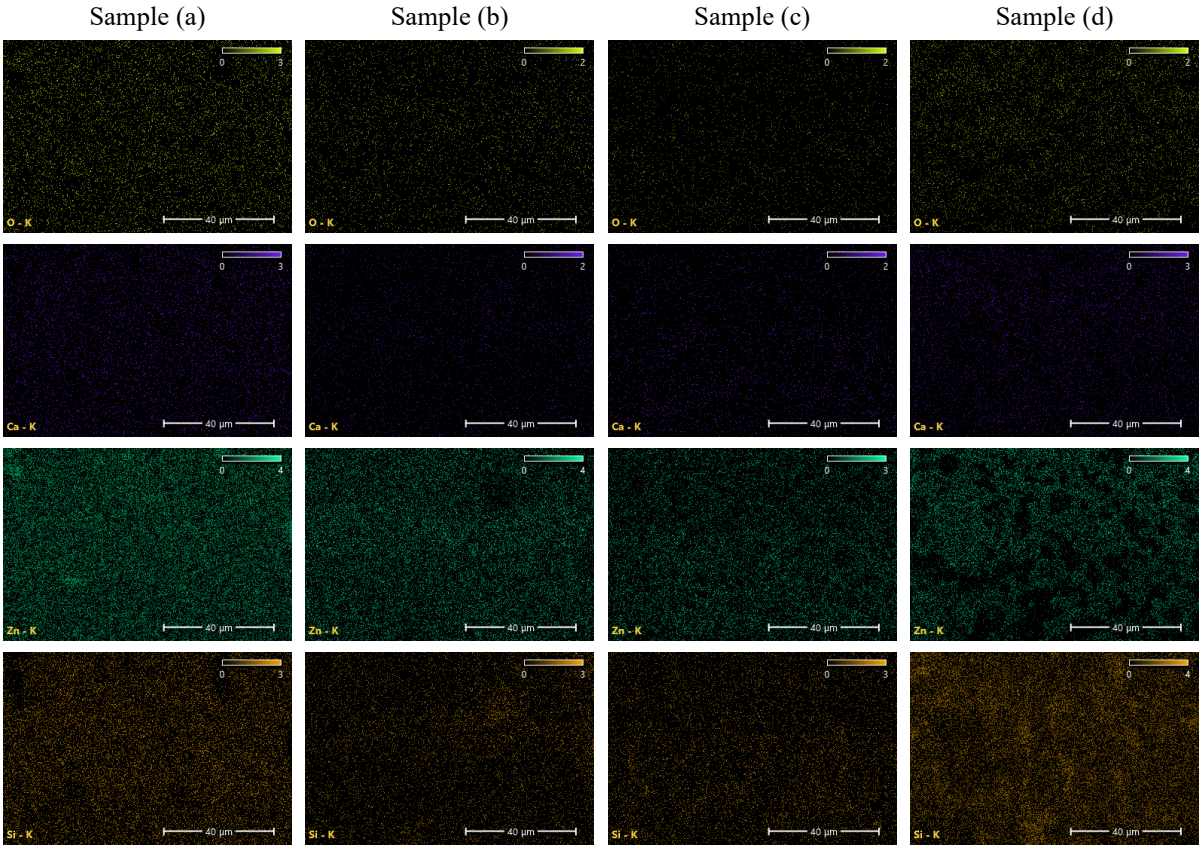

Fig. 8. EDX mapping of ZnO-seeded glass substrates prepared with different spacing from the evaporation crucible (a) 3 cm, (b) 4 cm, (c) 5 cm, and (d) 6 cm.

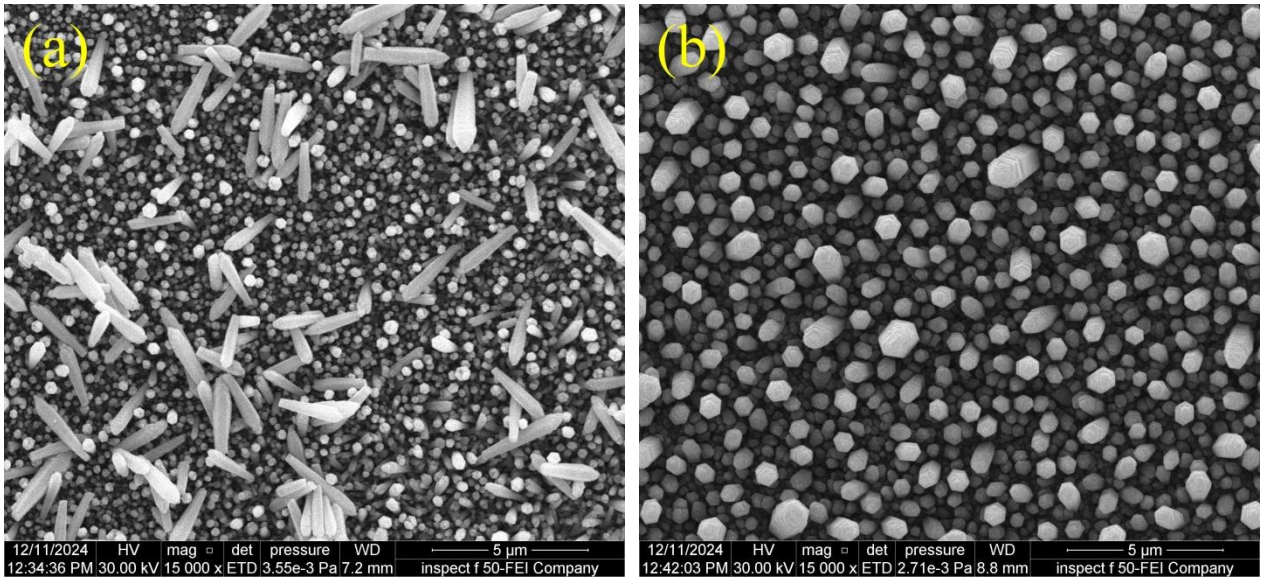

Fig. 9. FESEM images of the ZnO NRs grown (a) without, and (b) with seed layer with thickness of 178 nm.

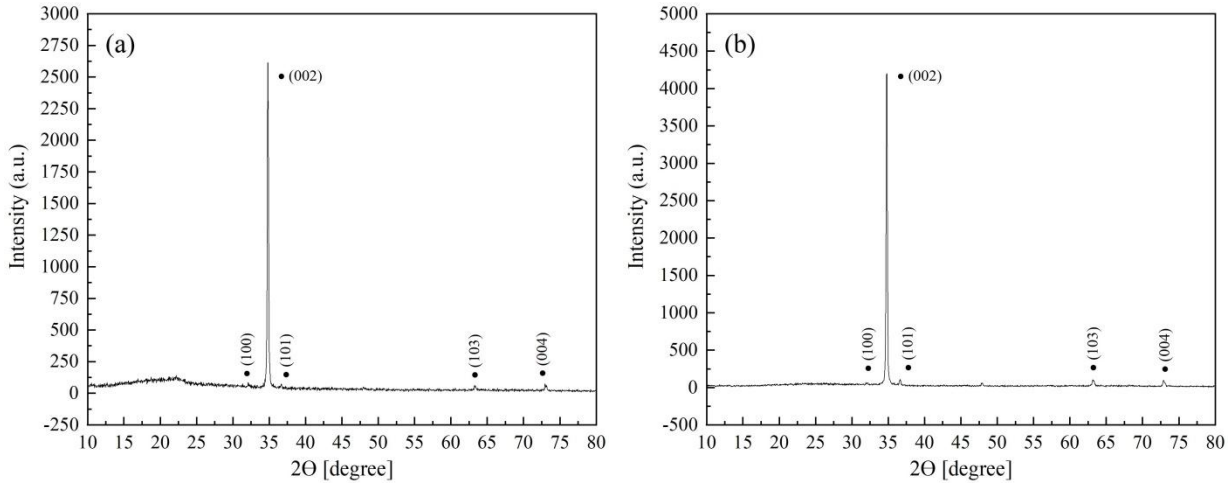

Fig. 10. XRD patterns of the ZnO NRs grown (a) without, and (b) with seed layer with thickness of 178 nm.

4. Conclusion

Utilizing a seeded layer-assisted chemical vapor deposition method, we synthesized vertically oriented ZnO NRs. This investigation explored the effects of changing the spacing between the evaporation crucible and the substrate (3, 4, 5, and 6 cm) on the optical performance, morphological attributes, and elemental structure of ZnO TFs formed as a seed layer. Moreover, the surface features of the fabricated ZnO NRs were examined in the presence and absence of the seed layer. It was shown that by adjusting the spacing, the blue shift in the UV absorption edge, E_g, and transmittance (~5-~80%) of the TFs could be organized. ZnO TFs have a direct optical E_g as decided by the Tauc formula. Analysis of the FESEM images reveals that the films prepared with a spacing of 6 cm exhibit uniformity, smoothness, transparency, and an absence of macroscopic defects, in contrast to those produced at other spacing. EDX spectroscopy analysis confirmed that all the films consisted mainly of Zn and O with high purity. FESEM images indicate that the presence of a seed layer can influence the growth behavior of the ZnO NRs. High crystallinity was verified in the samples through their XRD patterns, which showed a preferred growth direction along the (002) lattice plane. In conclusion, this study successfully achieved the growth of ZnO TFs with controlled thickness and favorable morphologies. These films are suitable for use as a seed layer (buffer layer) in the growth of 1D ZnO NSs in related research endeavors.

Acknowledgments

First and foremost, we would like to acknowledge the University of Mosul for its invaluable support and for allowing us the chance to engage in this academic venture.

Conflict of interest

The authors declare that they have no conflict of interest.

References

Jilani, A., Abdel-Wahab, M. S., and Hammad, A. H. (2017). Advance deposition techniques for thin film and coating. *Modern technologies for creating the thin-film systems and coatings*. 2(3), 137-149.

Płóciennik, P., Zawadzka, A., Frankowski, R., and Korcala, A. Selected methods of thin films deposition and their applications. *2016 18th International Conference on Transparent Optical Networks (ICTON)*: IEEE. 2016. 1-4.

Tu, K.-N. (2010). *Electronic Thin-Film Reliability*. Cambridge: Cambridge University Press.

Mohammed, Y. H., Sakrani, S. B., and Rohani, M. S. (2015). Improved structural features of Au-catalyzed silicon nanoneedles. *Superlattices and Microstructures*. 85(0), 849-858.

Rosli, A. B., Herman, S. H., Nordin, N. H., Mohd Sauki, N. S. a., Shariffudin, S., and Rusop Mahmood, M. (2014). Effect of seed layer morphology on the growth of zinc oxide nanotetrapods by thermal chemical vapour deposition method. *Advanced Materials Research*. 832, 429-433.

Saeed, Z. M., Mohammed, Y. H., and Ahmad, S. M. (2024). Atmospheric Pressure Chemical Vapor Deposition Grown One-Dimensional ZnO

Nanostructures. *Physics of the Solid State*. 66(7), 201-213.

Ahmad, I. A., and Mohammed, Y. H. (2023). Synthesis of ZnO nanowires by thermal chemical vapor deposition technique: Role of oxygen flow rate. *Micro and Nanostructures*. 181, 207628.

Sakrani, S., Jamaludin, N., Muhammad, R., Wahab, Y., Ismail, A. K., Suhaimi, S., and Mohammed, Y. H. (2016). Effect of gas flow rate on structural properties of zinc oxide nanowires grown by vapor-solid mechanism. *AIP Conference Proceedings*. 1733(1), 020040.

Chala, S., Sengouga, N., Yakuphanoğlu, F., Rahmane, S., Bdirina, M., and Karteri, İ. (2018). Extraction of ZnO thin film parameters for modeling a ZnO/Si solar cell. *Energy*. 164, 871-880.

Arya, S. K., Saha, S., Ramirez-Vick, J. E., Gupta, V., Bhansali, S., and Singh, S. P. (2012). Recent advances in ZnO nanostructures and thin films for biosensor applications. *Analytica chimica acta*. 737, 1-21.

Lee, P.-C., Hsiao, Y.-L., Dutta, J., Wang, R.-C., Tseng, S.-W., and Liu, C.-P. (2021). Development of porous ZnO thin films for enhancing piezoelectric nanogenerators and force sensors. *Nano Energy*. 82, 105702.

Sandeep, K., Bhat, S., and Dharmaprakash, S. (2017). Structural, optical, and LED characteristics of ZnO and Al doped ZnO thin films. *Journal of Physics and Chemistry of Solids*. 104, 36-44.

Shewale, P., and Yu, Y. (2017). UV photodetection properties of pulsed laser deposited Cu-doped ZnO thin film. *Ceramics International*. 43(5), 4175-4182.

Selim, M. S., Yang, H., Wang, F. Q., Fatthallah, N. A., Huang, Y., and Kuga, S. (2019). Silicone/ZnO nanorod composite coating as a marine antifouling surface. *Applied Surface Science*. 466, 40-50.

Shaida Anwar, K., Kurda, A. H., and Yousif Mawlood, H. (2024). Photodetector Devices: Investigation of ZnO Thin Films Fabricated via SILAR Technique on Various Substrates. *Zanco Journal of Pure and Applied Sciences*. 36(4), 24-32.

Park, D. J., Kim, D. C., Lee, J. Y., and Cho, H. K. (2006). Synthesis and microstructural characterization of growth direction controlled ZnOnanorods using a buffer layer. *Nanotechnology*. 17(20), 5238.

Banari, M., and Memarian, N. (2021). Effect of the seed layer on the UV photodetection properties of ZnO nanorods. *Materials Science and Engineering: B*. 272, 115332.

Paul, S., Das, A., Palit, M., Bhunia, S., Karmakar, A., and Chattopadhyay, S. (2016). Investigation of the properties of single-step and double-step grown ZnO nanowires using chemical bath deposition technique. *Adv. Mater. Lett*. 7, 610-615.

Ji, L.-W., Peng, S.-M., Wu, J.-S., Shih, W.-S., Wu, C.-Z., and Tang, I.-T. (2009). Effect of seed layer on the growth of well-aligned ZnO nanowires. *Journal of Physics and Chemistry of Solids*. 70(10), 1359-1362.

Yin, Y. T., Que, W. X., and Kam, C. H. (2010). ZnO nanorods on ZnO seed layer derived by sol–gel process. *Journal of Sol-Gel Science and*

Azmi, Z. H., Mohd Aris, S. N., Abubakar, S., Sagadevan, S., Siburian, R., and Paiman, S. (2022). Effect of seed layer on the growth of zinc oxide nanowires by chemical bath deposition method. *Coatings*. 12(4), 474.

Mohammed, Y. H., Sakrani, S. B., and Rohani, M. S. (2016). VHF-PECVD grown silicon nanoneedles: Role of substrate temperature. *Superlattices and Microstructures*. 91, 173-181.

Mohammed, Y. H. (2019). Fabrication of n-MgZnO/p-Si heterojunction diode: Role of magnesium doping. *Superlattices and Microstructures*. 131, 104-116.

Eckertová, L. (1977). *Physics of Thin Films*. New York: Springer US.

Soylu, M., and Savas, O. (2015). Electrical and optical properties of ZnO/Si heterojunctions as a function of the Mg dopant content. *Materials Science in Semiconductor Processing*. 29(Supplement C), 76-82.

26. Shinde, S. S., Shinde, P. S., Sapkal, R. T., Oh, Y. W., Haranath, D., Bhosale, C. H., and Rajpure, K. Y. (2012). Photoelectrocatalytic degradation of oxalic acid by spray deposited nanocrystalline zinc oxide thin films. *Journal of Alloys and Compounds*. 538, 237-243.

Singh, S. K., and Hazra, P. (2018). Performance analysis of undoped and Mg-doped ZnO/p-Si heterojunction diodes grown by sol–gel technique. *Journal of Materials Science: Materials in Electronics*. 29(6), 5213-5223.

Yahya, N. (2011). *Carbon and Oxide Nanostructures: Synthesis, Characterisation and Applications*. New York: Springer Berlin Heidelberg.

Kasap, S., and Capper, P. (2006). *Springer Handbook of Electronic and Photonic Materials*. NewYork: Springer.

Mortezaali, A., Taheri, O., and Hosseini, Z. S. (2016). Thickness effect of nanostructured ZnO thin films prepared by spray method on structural, morphological and optical properties. *Microelectronic Engineering*. 151, 19-23.

Mamat, M. H., Malek, M. F., Hafizah, N. N., Asiah, M. N., Suriani, A. B., Mohamed, A., Nafarizal, N., Ahmad, M. K., and Rusop, M. (2016). Effect of oxygen flow rate on the ultraviolet sensing properties of zinc oxide nanocolumn arrays grown by radio frequency magnetron sputtering. *Ceramics International*. 42(3), 4107-4119.

Guillén, C., and Herrero, J. (2010). Optical, electrical and structural characteristics of Al:ZnO thin films with various thicknesses deposited by DC sputtering at room temperature and annealed in air or vacuum. *Vacuum*. 84(7), 924-929.

Song, J., and Lim, S. (2007). Effect of seed layer on the growth of ZnO nanorods. *The Journal of Physical Chemistry C*. 111(2), 596-600.

Ghazali, M. N. I., Izmi, M. A., Mustaffa, S. N. A., Abubakar, S., Husham, M., Sagadevan, S., and Paiman, S. (2021). A comparative approach on One-Dimensional

ZnO nanowires for morphological and structural properties. *Journal of Crystal Growth*. 558, 125997.

Mohammed, Y. H., Sakrani, S. B., and Rohani, M. S. (2016). Pressure dependent tailored attributes of silicon nanoneedles grown by VHF plasma technique. *Superlattices and Microstructures*. 94, 147-157.

Mohammed, Y. H., Sakrani, S. B., and Rohani, M. S. (2016). Tunable morphological evolution of in situ gold catalysts mediated silicon nanoneedles. *Materials Science in Semiconductor Processing*. 50, 36-42.

Vasile, E., Plugaru, R., Mihaiu, S., and Toader, A. (2011). Study of microstructure and elemental micro-composition of ZnO: Al thin films by scanning and high resolution transmission electron microscopy and energy dispersive X-ray spectroscopy. *Romanian Journal of Information Science and Technology*. 14(4), 346-355.